Eur Radiol (2016) 26:3830–3839
DOI 10.1007/s00330-016-4248-z

CHEST

Diffusion weighted imaging in cystic fibrosis disease: beyond morphological imaging

Pierluigi Ciet[1,2,3] · Goffredo Serra[4] · Eleni Rosalina Andrinopoulou[5] · Silvia Bertolo[3] · Mirco Ros[6] · Carlo Catalano[4] · Stefano Colagrande[7] · Harm A. W. M. Tiddens[1,2] · Giovanni Morana[3]

Received: 2 November 2015 / Revised: 22 December 2015 / Accepted: 25 January 2016 / Published online: 12 February 2016

Abstract

Objectives To explore the feasibility of diffusion-weighted imaging (DWI) to assess inflammatory lung changes in patients with Cystic Fibrosis (CF)

Methods CF patients referred for their annual check-up had spirometry, chest-CT and MRI on the same day. MRI was performed in a 1.5 T scanner with BLADE and EPI-DWI sequences (b = 0–600 s/mm^2). End-inspiratory and end-expiratory scans were acquired in multi-row scanners. DWI was scored with an established semi-quantitative scoring system. DWI score was correlated to CT sub-scores for bronchiectasis (CF-CT$_{BE}$), mucus (CF-CT$_{mucus}$), total score (CF-CT$_{total\text{-}score}$), FEV$_1$, and BMI. T-test was used to assess differences between patients with and without DWI-hotspots.

Results Thirty-three CF patients were enrolled (mean 21 years, range 6–51, 19 female). 4 % (SD 2.6, range 1.5-12.9) of total CF-CT alterations presented DWI-hotspots. DWI-hotspots coincided with mucus plugging (60 %), consolidation (30 %) and bronchiectasis (10 %). DWI$_{total\text{-}score}$ correlated (all $p < 0.0001$) positively to CF-CT$_{BE}$ (r = 0.757), CF-CT$_{mucus}$ (r = 0.759) and CF-CT$_{total\text{-}score}$ (r = 0.79); and negatively to FEV$_1$ (r = 0.688). FEV$_1$ was significantly higher ($p < 0.0001$) in patients without DWI-hotspots.

Conclusions DWI-hotspots strongly correlated with radiological and clinical parameters of lung disease severity. Future validation studies are needed to establish the exact nature of DWI-hotspots in CF patients.

Key Points

- *DWI hotspots only partly overlapped structural abnormalities on morphological imaging*
- *DWI strongly correlated with radiological and clinical indicators of CF-disease severity*
- *Patients with more DWI hotspots had lower lung function values*
- *Mucus score best predicted the presence of DWI-hotspots with restricted diffusion.*

Keywords Magnetic resonance imaging · Diffusion magnetic resonance imaging · Cystic fibrosis · Pulmonary inflammation · Disease exacerbation

Electronic supplementary material The online version of this article (doi:10.1007/s00330-016-4248-z) contains supplementary material, which is available to authorized users.

✉ Giovanni Morana
gmorana@ulss.tv.it

1 Department of Radiology, Erasmus Medical Center, Rotterdam, Netherlands

2 Department of Paediatrics, Respiratory Medicine and Allergology, Erasmus Medical Center - Sophia Children's Hospital, P.O. Box 2060, Wytemaweg 80, Rotterdam 3000 CB, Zuid-Holland, Netherlands

3 Department of Radiology, Ca' Foncello - General Hospital, Piazzale Ospedale, 1, 31100 Treviso, Italy

4 Department of Radiology, University of Rome "Sapienza", Rome, Italy

5 Department of Biostatistics, Erasmus Medical Center, Rotterdam, The Netherlands

6 Department of Pediatrics, Ca' Foncello Hospital, Treviso, Italy

7 Department of Experimental and Clinical Biomedical Sciences, Radiodiagnostic Unit n. 2, University of Florence - Azienda Ospedaliero-Universitaria Careggi., Largo Brambilla 3, Florence 50134, Italy

Introduction

Cystic Fibrosis (CF) lung disease is characterized by chronic airways infection, inflammation, and progressive lung damage

starting in early childhood [1]. Exacerbations, and acute episodes of infection and inflammation, eventually lead to end-stage lung disease, the main cause of death in patients with CF [2]. Regular monitoring that includes a physical examination, spirometry, quality-of-life questionnaires and imaging [3], is used to detect lung changes that require timely treatment [4].

To date, imaging techniques such as chest x-ray (CXR) and chest-CT (CT) have been the preferred methods for CF monitoring; however, both techniques have limitations [5]. CXR only allows detection of gross lung changes, such as consolidation, atelectasis, and pleural effusion [5]. CT is far more sensitive to localize and quantify structural changes [6]; however, short-term follow-up with CT, for example during an exacerbation, is restricted by radiation exposure [7]. The latter limitation was the driving force to introduce MRI in CF lung monitoring [8]. Unfortunately, MRI has inferior sensitivity compared to CT to detect structural changes in the CF lung [9, 10] due to a lower spatial resolution. However, more recently the resolution has improved by using newly developed sequences, such as ultrashort [11] or zero echo time [12]. Furthermore, the interest for using MRI in CF has expanded towards functional imaging [13]. Multi-parametric MRI, such as Fourier Decomposition [14], hyperpolarized-gases MRI, and oxygen-enhanced MRI [15, 16], provide information not readily available with CT [17]. Diffusion-weighted imaging (DWI) is another MRI technique that might have great potential in CF lung monitoring [18]. To date, DWI has been primarily used to assess malignancies in thoracic imaging [19]. Interestingly, DWI has proved to be accurate in the identification of inflammation in various organs, such as brain, spine, muscle, and intestines [20–23]. Based on these studies, we investigated whether DWI has potential to detect inflammatory changes in CF lung disease.

The main aims of our study were: 1) to explore the feasibility of DWI to detect lung inflammatory changes in CF patients, and 2) to correlate DWI with radiological and clinical indicators of CF lung disease severity.

Material and methods

In this multicenter prospective cross-sectional study, patients with CF scheduled for their routine annual evaluation were consecutively recruited in two Italian CF centres (Treviso and Rome) by their treating physicians. At the clinical evaluation, each patient was informed about the study and asked to participate. When willing to participate, the subject was scheduled for the study protocol within two weeks from the visit. The study was approved by the institutional review board in all participating centres (n. 292/AULSS9 and n. 419/09). All patients underwent a physical examination, spirometry, chest-CT, and chest-MRI on the same day. Inclusion and exclusion criteria are described in Table 1.

Physical examination and spirometry

Informed consent was obtained, and each patient underwent a clinical examination, pulse oximetry, and spirometry, prior to imaging. As part of the clinical exam, heart and respiratory rate, weight and height were recorded. Spirometry was performed according to the ATS/ERS guidelines [24].

CT and MRI protocol

The routine biennial CT protocol consisted of volumetric end-inspiratory and end-expiratory low-dose scans in a 16- or 64-row scanner (SOMATOM Sensation, Siemens, Erlangen, Germany) using the following parameters: 120 kV for patients ≥ 35 kg,100 kV for patients < 35 kg, mAs 15–40, no contrast agent, 1 mm collimation, slice thickness 1 mm, reconstruction increment 0.8 mm, pitch 1. Five mm axial and coronal reformats with kernels B31f, B60f, and B70f were obtained to match the slice thickness of MR images.

In addition to the routine CT protocol a chest MRI was performed on the same day. The MRI protocol consisted of respiratory-triggered scans using a 16 channel torso coil in a clinical 1.5 T scanner, with the following parameters: axial and coronal BLADE sequence proton-density (PD)-weighted with navigator (TR/TE/alpha/: ∞/28 ms/90°, in plane resolution 1.2 × 1.2 mm and slice thickness 5 mm) and T2-weighted axial BLADE sequence (TR/TE/alpha = 2000 ms/27 ms/150°, in plane resolution 3.2 × 2.5 mm and slice thickness 5 mm). DWI was acquired using a single-shot echo-planar imaging sequence (EPI) in the axial plane, with gradients equal in all directions (readout, phase, and slice-section orientations). DWI was obtained with b values of 0 and 600 s/mm^2 (TR/TE/alpha = 5632 ms/83 ms/90°, slice thickness 5 mm, gap 0 mm, 2 average). All sequences were acquired at end-expiration during free-breathing using navigator echoes respiratory triggering. The MRI protocol was identical in both CF centres, which had the same MRI scanner (MAGNETOM Avanto, Siemens Healthcare, Erlangen, Germany).

Image analysis

All CT and MRI images were anonymized and evaluated in random order by two radiologists (P.C. and G.S.), with 4 years and 1 year of experience in thoracic CT and MRI scoring, respectively. Both radiologists were blinded to any clinical information and to each other's CT and MRI assessment. Prior to this study, both radiologists were trained in the CF center of Erasmus MC (Rotterdam, the Netherlands) to the CF-CT and CF-MRI scoring systems [25], which were used to score the CT and BLADE MR images [26].The total score is the sum of the individual sub-scores per lobe of the following

Table 1 Inclusion / Exclusion criteria for patient selection

Inclusion criteria	Exclusion Criteria
• Proven CF as evidenced by positive sweat test or two CF gene mutations • Scheduled for biennial routine chest-CT scan requested by the attending physician • Ability to perform reproducible maneuvers for spirometry • Ability to comply with instructions during CT and MRI examinations	• Age below 6-years • Chronic oxygen therapy • Present or recent (two weeks) pulmonary exacerbation • History of lung transplantation • Participation in another trial • Contraindications for MRI • Proved or possible pregnancy • Not able or not willing to give informed consent

parameters: bronchiectasis (CF-CT_{BE}); mucus plugging (CF-CT_{mucus}); air wall thickening (CF-CT_{AWT}); trapped air (CF-CT_{TA}), and parenchyma (CF-CT_{PAR}) [26]. Sub-scores and total scores are expressed as % of the maximal possible score.

DWI images were scored in random order using a semi-quantitative scoring approach, which has been used in previous studies [27–29]. This qualitatively analyzes the signal intensity of lung lesions with altered signal intensity (hotspots). Each hotspot was visually graded on a three-point score scale by signal intensity: score 0, no signal; score 1, weak signal and score 2, strong signal. Signal intensity was judged using the highest b-value (b = 600 s/mm^2) images, compared to the signal of the spinal cord. Spinal cord was used as the reference structure as it has constant high signal intensity on high b values as a result of the anatomical organization of the sagittal nerve fascicles, and it is alongside the entire chest. When the DWI signal of lung parenchymal hotspots was lower than that of the cord, it was graded as "weak" ($DWI_{weak\ score}$, score = 1), whereas if the signal was greater than or equal to that of the cord it was graded as "strong" ($DWI_{strong\ score}$, score = 2). The total DWI score ($DWI_{total\ score}$) is the sum of all weak and strong hotspots for each of the six lung lobes, with lingula considered a separate lobe. A quantitative analysis was not performed based on the poor reliability of the apparent diffusion coefficient (ADC) maps due to residual motion and susceptibility-induced distortions. Following DWI scoring, using fusion technique (Image Fusion, Siemens Healthcare, Erlangen, Germany) between DWI and correlated morphological image (axial BLADE), the anatomical substrate and the distribution of the DWI hotspots was identified. In uncertain cases, the CT was used as reference image. The percentage of structural CT changes presenting hotspots in DWI images was computed as a ratio between the $DWI_{total\ score}$ and the CF-$CT_{total\ score}$. Anatomical substrates with DWI signal were categorized in a similar fashion to the CF-CT and CF-MRI scoring system (Online supplement digital content 1).

Statistical analysis

For each patient, the mean DWI score of the two observers was used to assess frequency and distribution of the anatomical substrates with DWI signal. Inter-observer agreement for the CF-CT, CF-MRI, and DWI scoring methods was assessed using the intraclass correlation coefficient (ICC) and Bland-Altman plots. ICC values between 0.40-0.60; 0.60-0.80; and ≥ 0.80 are considered to represent moderate, good, and very good agreement, respectively.

Pearson's correlation was used to measure the strength of the association between DWI score and clinical and radiological parameters reflecting disease severity. These parameters included: forced expiratory volume in one second (FEV_1 % predicted); Body Mass Index (BMI); CF-CT_{BE}; CF-CT_{mucus}; and CF-$CT_{total\ score}$. According to Cohen's criteria,

Table 2 Patients' characteristics

	Mean	Standard deviation	Range
Clinical parameters			
BMI (kg/m^2)	19.1	3.4	12.9-29.9
FEV_1 % predicted	71.8	25.2	24-113.4
CT scores			
CT-BE (%)	22.4	10.6	3.5-43.8
CT-Mucus (%)	21.7	13.7	0-44.4
CF-CT (%)	25.1	11.6	2.7-45.1
DWI scores			
Weak DWI score	6.0	5.2	0-17.5
Strong DWI score	6.9	8.4	0-32
Total DWI score	20.4	14.0	1-54

BMI=Body Mass Index, CT-BE= Computed tomography bronchiectasis sub-score, CF-CT=Cystic Fibrosis Computed Tomography score, CT-Mucus= Computed tomography mucus plugs sub-score, DWI= Diffusion Weighted Imaging, FEV_1%=Forced expiratory volume in one second % predicted. All CT score and sub-scores are expressed as a percentage of the maximum possible score, ranging from 0 (no pathological findings) to 100 (maximum severity). The maximum possible scores for CF-CT, CT-BE and CT-mucus sub-scores are 243, 72, and 36, respectively. DWI scores are expressed as mean score of the two observers for each patient

correlations with r between 0.10 and 0.29 are considered weak, between 0.30 and 0.49 moderate and above 0.50 are strong [30]. Multiple comparisons were adjusted using the Bonferroni correction. Differences in continuous variables between patients with and without DWI hotspots were examined using a Student t-test.

Finally, data were analyzed using a mixed-effects models to investigate whether there was an association between specific covariates and the outcomes of interest, while accounting for the correlation within the same patients [31]. The covariates tested in the model were BMI, FEV_1, sex, CF-$CT_{BE,}$ CF-CT_{mucus} and score of each observer (score observer 1 versus

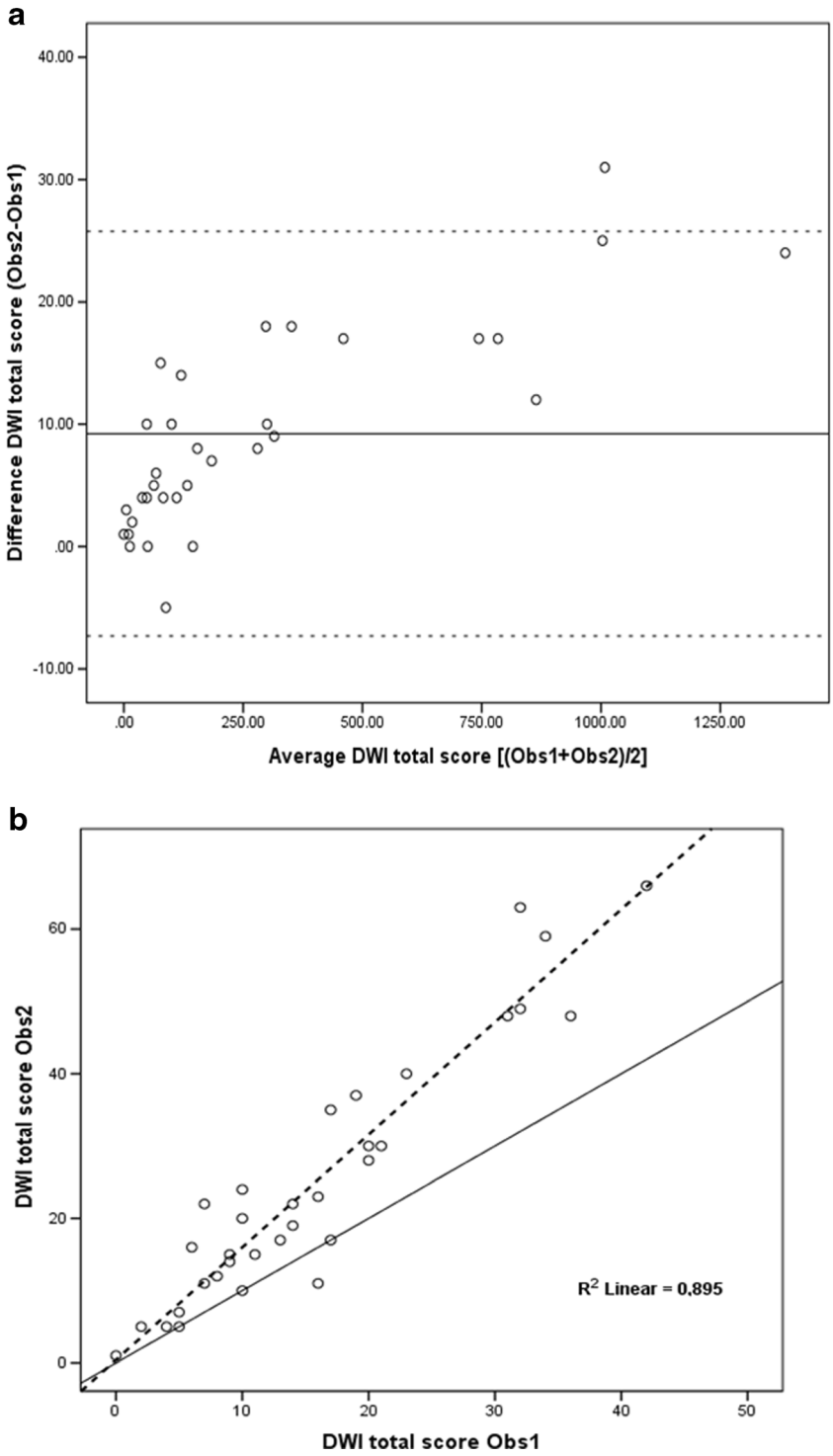

Fig. 1 **a** Bland-Altman for Total DWI score observer 1 (Obs1) versus observer 2 (Obs2). Thick line is the mean, dashed lines are ± 2 standard deviations (SD). **b** Identity Plot Total DWI score observer 1 versus observer 2. The continuous line is the identity line (y = 1*x + 0), dashed line is the correlations line. Note that observer 2 had higher scores than observer 1 (mean difference ~ 9)

observer 2). The outcome tested for these covariates were: $DWI_{weak\ score}$, $DWI_{strong\ score}$, and $DWI_{total\ score}$. The Akaike information criterion (AIC) was used to investigate which model performs better [32]. The lowest AIC coefficient defines the best model for the given data, and differences in AIC coefficient greater than 5 points are considered significant [32]. Differences were statistically significant if $p < 0.05$. Statistical analysis was performed with SPSS (version 20.0, SPSS, Chicago, IL, USA) and R (version 3.1.3, the R foundation for statistical computing, Vienna, Austria).

Results

After 12 months of recruitment (April 2011- March 2012) period, thirty-eight consecutively selected patients with CF (mean age 24 years, range 6–51 years, 22 females) were enrolled in the study. Five subjects were excluded for incomplete study protocol, so eventually thirty-three patients with CF were used for data analysis. (mean age 21 years, range 6–51 years, 19 females). Patients' characteristics, CT and DWI scores are summarized in Table 2.

Distribution and anatomical substrates of DWI signal

A mean number of 6 (SD 5.2, range 0–17.5) weak and 6.9 (SD 8.4, range 0–32) strong DWI hotspots were identified. DWI hotspots were distributed in decreasing order in the right upper lobe (mean 25.4 %, SD 8.4, range 0–37.9 %), right lower lobe (mean 24.7 %, SD 6.8, range 16.3-50 %), left lower lobe (mean 21.5 %, SD 6.9, range 10–36.7 %), left upper lobe (mean 13.5 %, SD 3.6, range 6.7-20.6 %), right middle lobe (mean 8.2 %, SD 5.4, range 0–18.2 %) and lingula (mean 6.7 %, SD 3.1, 1.5-13.3 %). The most frequent structural lung alterations as examined on axial BLADE with either weak or strong DWI signal were mucus plugging (mean 61 %, SD 35, range 0–100 %), followed by consolidation (mean 26.5 %, SD 16.8, range 0–54 %), and bronchiectasis (mean 12.5 %, SD 9.3, range 0–37.5 %). The DWI hotspots pattern only partially overlapped the structural lung changes on morphological MRI or CT, and only 4 % (SD 2.6, range 1.5-12.9 %) of total CF-CT structural lung changes presented DWI hotspots.

Reliability of DWI score

Overall, inter-observer agreement for CF-CT and CF-MRI sub-scores was good or very good, except for the trapped-air sub-score. ICCs for CF-CT and CF-MRI are presented as a table in the online supplement digital content 2[BLINDED]. Inter-observer agreements for $DWI_{weak\ score}$, $DWI_{strong\ score}$, and $DWI_{total\ score}$ were good: ICC 0.76 (C.I. 95 %, 0.55-0.87), 0.74 (C.I. 95 %, 0.43-0.87) and 0.7 (C.I. 95 %, 0.04-0.89), respectively. Bland-Altman and identity plots showed that observer 2 had systematically higher $DWI_{total\ score}$ scores than observer 1 (Fig. 1). Bland-Altman and identity plots for total DWI hotspots identified by each observer are presented as online supplement digital content 3.

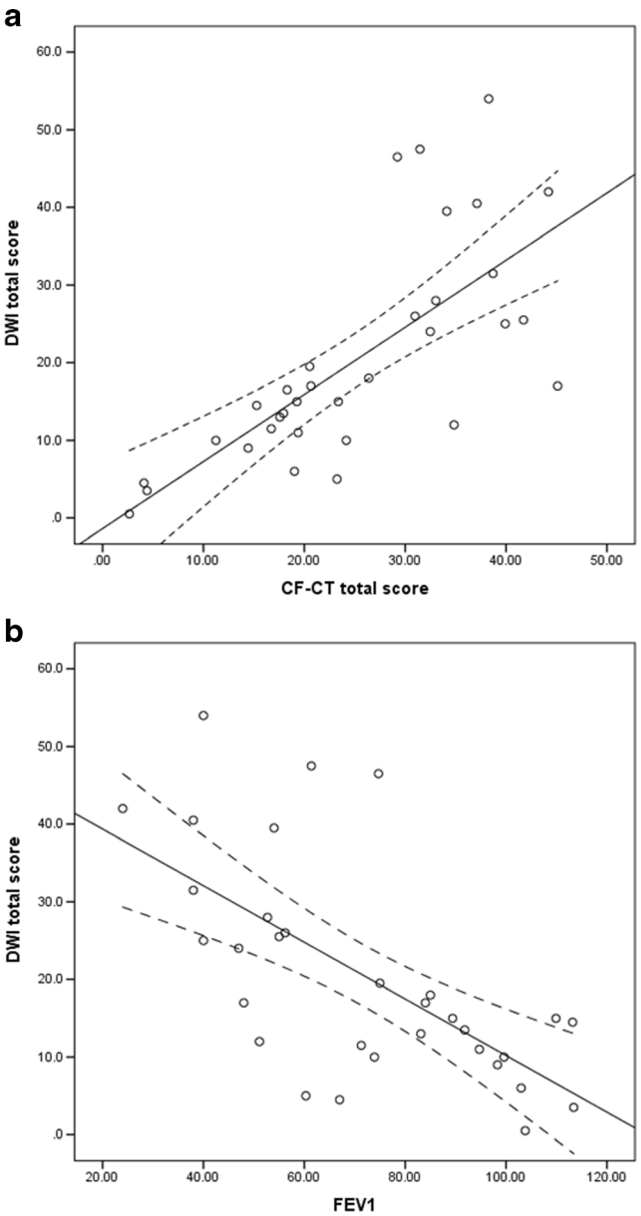

Fig. 2 **a** Correlation of total diffusion weighted imaging (DWI) score with total cystic fibrosis computed tomography score (CF-CT score). **b** Correlation of total DWI score with forced expiratory volume in 1 second (FEV_1). Continuous lines are correlation lines, dashed lines are 95 % confidence intervals. Note strong positive correlation of total DWI score with total CF-CT score (Pearson $r = 0.717$, $p < 0.0001$), and strong negative correlation with FEV_1 (Pearson $r = -0.649$, $p < 0.0001$). Mean score of the two observers was used to build the plots

Correlations of DWI signal with clinical and radiological parameters

Total DWI score had strong positive correlation with CF-CT_{BE} ($r=0.757$ observer 1, $r=0.510$ observer 2), CT_{mucus} ($r=0.759$ observer 1, $r=0.584$ observer 2) sub-scores, and CF-$CT_{total\ score}$ ($r=0.790$ observer 1, $r=0.618$ observer 2) (Fig. 3). $DWI_{total\ score}$ had strong negative correlation with FEV_1 ($r=-0.688$ observer 1, $r=-0.611$ observer 2) (Fig. 2): FEV_1 in patients without DWI hotspots ($n=11$) was significantly higher ($p<0.0001$) than those of patients with DWI hotspots. BMI did not correlate with $DWI_{total\ score}$ and no significant differences in BMI were found between the groups with or without hotspots.

Relationship of covariates in DWI scores: mixed-effects models

For the DWI_{strong} outcome, the model with the covariate CF-CT_{mucus} (AIC = 398.6) was better than the model with FEV_1 (AIC = 406.2). However, there were no significant differences in AIC coefficient between the model with FEV_1 or CF-CT_{mucus} covariates when tested for the DWI_{weak} and $DWI_{total\ score}$ outcomes (DWI_{weak}: AIC-FEV_1 = 367.4, AIC-CF-CT_{mucus} = 368; $DWI_{total\ score}$: AIC-FEV_1 = 447, AIC-CF-CT_{mucus} = 446.9). Therefore, we considered the best predictive model for all three DWI outcomes (weak, strong, and total DWI) that including CF-CT_{mucus} but not FEV_1. The final model included the covariates: BMI, gender, observer score, CF-CT_{BE}, and CF-CT_{mucus}. In this model the CF-CT_{mucus} and observer score covariates were significant for the DWI_{strong}, and for $DWI_{total\ score}$. For the $DWI_{weak\ score}$ outcome, the CF-CT_{BE} covariate was significant, while CF-CT_{mucus} tended to be significant ($p=0.052$). Mixed-effects models results are summarized in Table 3. Figure 3 shows effect plots for each DWI score outcome ($DWI_{weak\ score}$, $DWI_{strong\ score}$, and $DWI_{total\ score}$) based on the mixed-effects model analysis.

Discussion

To our knowledge, this is the first study that has used DWI to assess CF lung disease, and several observations can be made from these results.

The most important observation is that DWI hotspots only partially overlapped the structural lung changes as seen on morphological CT or MRI (Fig. 4). Moreover, the DWI signal for the same parenchymal abnormality on MRI in a single patient was very different. For instance, mucous plug as observed on MRI in a lobe could show different signal intensities, from no signal to a very intense signal (Fig. 5). Similar variability was also observed for other structural lung changes, such as consolidation and bronchiectasis, which were the most frequent structural lung changes presenting a DWI signal. We speculate that the observed differences in DWI signal intensity might be related to the severity of local inflammation, based on differences in the cellularity of the structure examined and consequently in differences in the restriction of proton movement.

Alternative explanations are that increased DWI signal intensity depend on an increased capillary perfusion in relation to inflammation, which can be detected by DWI as D* (pseudo-diffusion coefficient) associated with blood flow [33]. However, pseudo-diffusion was not assessed in our MRI protocol, as intravoxel incoherent motion imaging was not applied [34]. Furthermore, differences in DWI signal intensity (weak vs. strong) among the structural lung changes could be related to differences in water concentrations caused by T2-shine-through artefact [35]. To overcome this, we assessed

Table 3 Effect table for DWI scores outcomes based on the mixed-effects models analysis

	$DWI_{weak\ score}$			$DWI_{strong\ score}$			$DWI_{total\ score}$		
	Value	SE	p-value	Value	SE	p-value	Value	SE.	p-value
Intercept	−1.5241	4.0634	0.7102	8.6896	4.3673	0.0558	16.3902	6.5247	0.0176*
Observer score	−0.6208	0.7530	0.4162	−3.0626	1.1507	0.0124*	−8.2908	1.6539	<0.0001*
BMI	0.0389	0.2011	0.8480	−0.3395	0.1976	0.0960	−0.1354	0.2905	0.6445
Gender	1.3513	1.3371	0.3203	−0.3958	1.3170	0.7658	0.6968	1.9399	0.7220
CF-CT_{BE}	0.1736	0.0705	0.0197*	0.0645	0.1029	0.5355	0.2021	0.1485	0.1836
CF-CT_{mucus}	0.1113	0.0551	0.0524	0.2304	0.0597	0.0006*	0.2660	0.0831	0.0032*

BMI= Body Mass Index, CF-CT_{BE}=Computed tomography bronchiectasis score, CF-CT_{mucus}= Computed tomography mucus score, FEV_1= Forced expiratory Volume in 1 second % of predicted, SE= Standard Error. Note significant differences in observer score (scores observer 1 vs. observer 2) and CF-CT_{mucus} covariates for $DWI_{strong\ score}$ and $DWI_{total\ score}$ outcomes (*). For the $DWI_{weak\ score}$ outcome, the CF-CT_{BE} is significant (*), while CF-CT_{mucus} tends to be significant

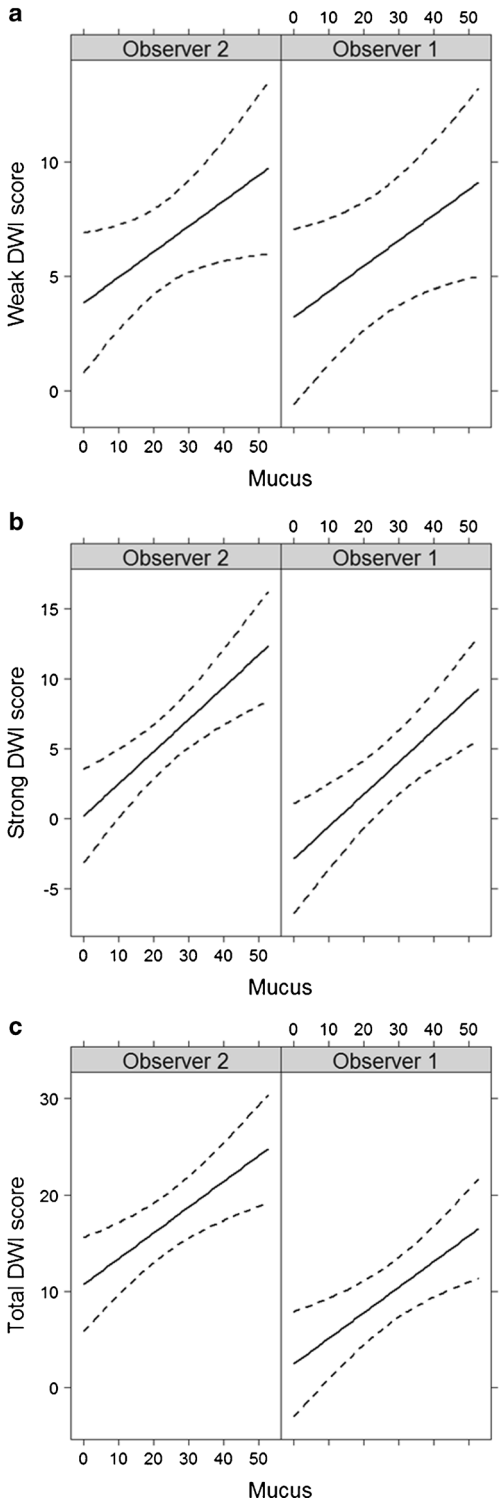

Fig. 3 Effects plots for diffusion-weighted imaging (DWI) scores outcomes (**a**) weak, (**b**) strong, and (**c**) total DWI score; and CF-CT_{mucus} covariate. Each plot has two curves, one for each observer. Y-axis represents DWI scores while x-axis the CF-CT_{mucus} sub-score expressed as % of maximum score, which is 36 for mucus. Each plot simulates changes in CF-CT_{mucus} sub-score according DWI scores for patients with mean BMI, mean CF-CT_{BE} sub-score and male gender. For instance, an increase of about 10 % in CF-CT_{mucus} sub-score (**c**) produces an increase of $DWI_{total\ score}$ of almost 3 points. Note that, although observer 2 has overall higher total DWI scores (**c**); the slope of the relation between $DWI_{total\ score}$ and CF-CT_{mucus} sub-score is the same as for observer 1

and scored the DWI images in the highest b-value (b = 600 s/mm^2), with reduced T2-shine-through effect (Fig. 5).

The second important finding is that DWI scores correlated well with radiological and clinical indicators of CF lung disease severity. DWI scores had a strong positive correlation with CF-CT score and a moderate negative correlation with FEV_1. In particular, the higher the DWI score, the higher the CF-CT score, or the lower the FEV_1. These correlations suggest that patients with more severe CF lung disease have a larger number of DWI hotspots. This observation is also supported by the findings that there were significant differences in FEV_1 between patients with and without DWI hotspots.

The third important observation is from the mixed-effects model, which shows that for the DWI_{strong} outcome, the best model (lowest AIC coefficient) was the model that included the CF-CT_{mucus} sub-score instead of the FEV_1 covariate. DWI_{strong} score represents those hotspots with high DWI signal, which suggests a restricted diffusion. Paired with the finding that mucus was also the most frequent alteration associated with DWI signal, it suggests that mucus significantly contributes to the "inflammatory" DWI hotspots in CF lung disease. This is not unlikely as reduced mucus clearance is considered to be the primary cause of chronic airway infection and inflammation in CF [1].

We acknowledge some limitations to this study. First, we used a semi-quantitative scoring system to assess DWI signal and did not compute ADC maps. The main reason was that the ADC maps were not reliable due to residual motion and susceptibility-induced distortions. Part of these distortion artefacts was counterbalanced by doubling the number of averages during image acquisition. More than two averages combined with respiratory-triggered acquisition were not feasible, as it would have led to unacceptably long acquisition times of the DWI sequence (>10 minutes). For these reasons, we used a semi-quantitative approach that has proved to be reliable in previous studies, with high sensitivity and specificity [29]. Moreover, this method showed good agreement between the observers.

Second, there were significantly different scores between the observers as shown by the Bland-Altman plots and by the mixed model analysis (observer score covariate). However, correlations using the individual

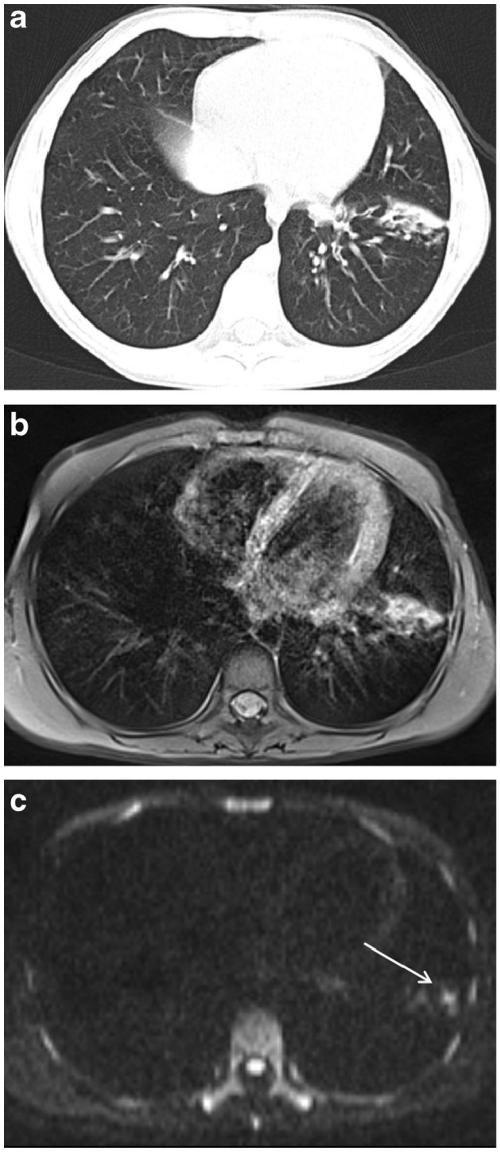

Fig. 4 **a** End-inspiratory axial CT, **b**) Free-breathing PD-weighted axial BLADE image, and **c**) diffusion-weighted imaging (DWI) free breathing (**b** = 600 s/mm^2). Note that DWI signal (hotspot) only partially overlaps the left lower lobe consolidation, with the most peripheral portion presenting the highest signal (arrow). This indicates that the lesion has non-homogenous DWI characteristics, with the most peripheral portion having more restricted diffusion

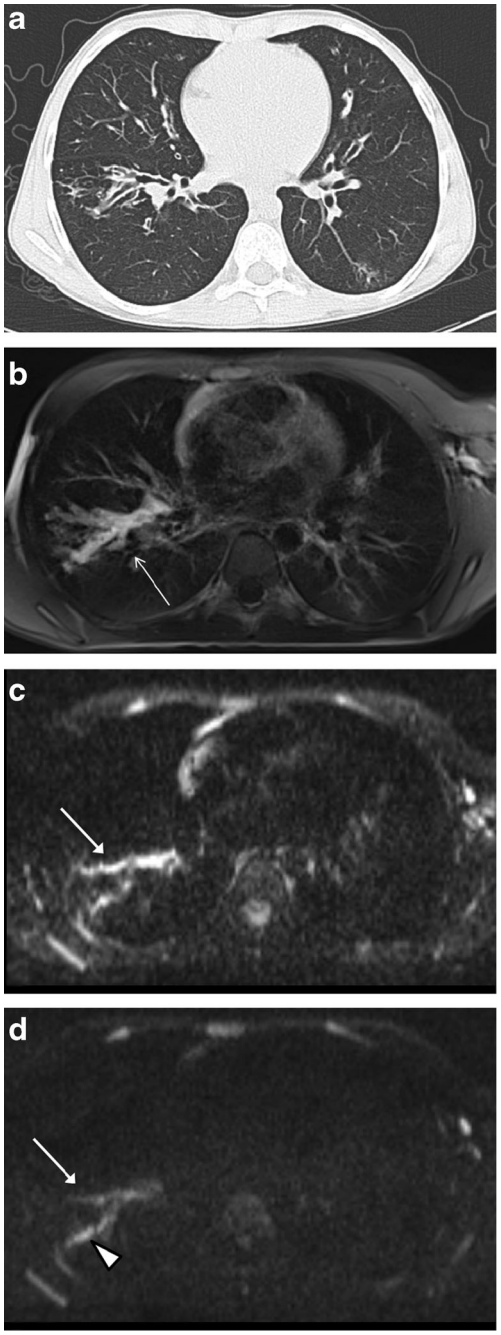

Fig. 5 **a** End-inspiratory axial CT, **b**) free-breathing PD-weighted axial BLADE image, **c**) Diffusion Weighted Imaging (DWI) free breathing (**b** = 0 s/mm^2) and D) DWI (**b** = 600 s/mm^2). A large bronchiectasis filled with mucus can be appreciated in the right lower lobe (arrow in **b**) Note heterogeneous DWI signal decay in highest b-value of the mucus-filled bronchiectasis (arrow in **c** and **d**), although it persists in the dorsal branch due to persistent restricted diffusion (arrowhead in **d**)

scores of each observer instead of taking the mean scores of both observers obtained the same significant and concordant results (Table 3). Hence, it is unlikely that the differences in scores between the observers had any impact on our most important findings. The development of a fully quantitative approach will overcome this inter-observer limitation, by providing objective ADC maps that are independent of observer variability. For now, we are improving the image quality of our DWI protocol, to facilitate the use of ADC maps for future studies.

Finally, we did not objectively assess the exact nature of these DWI hotspots. However, our study had the main aim to investigate the information obtainable with DWI in CF lung disease. Clearly, further studies are needed to validate this technique in CF patients suffering from a pulmonary tract exacerbation.

Conclusions

In summary, this study is the initial exploratory phase towards the development of DWI as a technique to quantify lung inflammation in CF lung disease. We observed that the DWI hotspots pattern only partly overlapped structural abnormalities on morphological CT or MRI. In addition, DWI scores had a strong correlation with radiological and clinical indicators of CF lung disease severity. Significant differences in pulmonary function (FEV_1) were found between patients without and with DWI hotspots. Finally, we found that the amount of mucus in patients with CF was the best predictor of strong DWI hotspots (restricted diffusion).

These compelling results have established the foundations for future validation studies in CF patients with pulmonary exacerbation, to establish the exact nature of these DWI hotspots.

Acknowledgments The authors thank Elizabeth Salamon, Department of Respiratory Medicine, Royal Perth Hospital, for offering invaluable detailed advice on grammar and organization of the manuscript. The authors also thank Thorsten Feiweier, Siemens Healthcare Erlangen, Germany, for technical advice in critically reviewing the manuscript. The researchers also wish to express their deepest gratitude to all CF patients, who participated in the study.

The scientific guarantor of this publication is Dr. Giovanni Morana, chief of the Radiology Department at Ca'Foncello General Hospital, Treviso, Italy. The authors of this manuscript declare relationships with the following companies: Bracco Imaging (not related to this article). The authors of this manuscript declare no other relationships with any companies, whose products or services may be related to the subject matter of the article. This study has received funding by the Italian cystic fibrosis league *(Lega Italiana Fibrosi Cistica, LIFC)* to cover the travel expenses of the first author.

Eleni Rosalina Andrinopoulou, statistician, kindly provided statistical advice for this manuscript. Institutional Review Board approval was obtained in all participating centres. Written informed consent was obtained from all subjects (patients) in this study. Study subjects have been previously reported in *Assessment of CF lung disease using motion corrected PROPELLER MRI: a comparison with CT. European Radiology DOI: 10.1007/s00330-015-3850-9*. Methodology: prospective, cross sectional study, observational, multicenter study.

References

1. Tiddens HAWM, Donaldson SH, Rosenfeld M, Paré PD (2010) Cystic fibrosis lung disease starts in the small airways: can we treat it more effectively? Pediatr Pulmonol 45:107–117
2. Loeve M, Gerbrands K, Hop WC et al (2011) Bronchiectasis and pulmonary exacerbations in children and young adults with cystic fibrosis. Chest 140:178–185
3. Conway S, Balfour-Lynn IM, De Rijcke K et al (2014) European cystic fibrosis society standards of care: framework for the cystic fibrosis centre. J Cyst Fibros 13:S3–S22
4. Grasemann H, Ratjen F (2013) Early lung disease in cystic fibrosis. Lancet Respir Med 1:148–157
5. Eichinger M, Heussel C-P, Kauczor H-U et al (2010) Computed tomography and magnetic resonance imaging in cystic fibrosis lung disease. J Magn Reson Imaging 32:1370–1378
6. Loeve M, Hop WCJ, De Bruijne M et al (2012) Chest computed tomography scores are predictive of survival in patients with cystic fibrosis awaiting lung transplantation. Am J Respir Crit Care Med 185:1096–1103
7. Kuo W, Ciet P, Tiddens HAWM et al (2014) Monitoring cystic fibrosis lung disease by computed tomography. Radiation risk in perspective. Am J Respir Crit Care Med 189:1328–1336
8. Wielpütz MO, Eichinger M, Puderbach M (2013) Magnetic resonance imaging of cystic fibrosis lung disease. J Thorac Imaging 28: 151–159
9. Failo R, Wielopolski PA, Tiddens HAWM et al (2009) Lung morphology assessment using MRI: a robust ultra-short TR/TE 2D steady state free precession sequence used in cystic fibrosis patients. Magn Reson Med 61:299–306
10. Ciet P, Serra G, Bertolo S et al (2015) Assessment of CF lung disease using motion corrected PROPELLER MRI: a comparison with CT. Eur Radiol. doi:10.1007/s00330-015-3850-9
11. Ma W, Sheikh K, Svenningsen S et al (2015) Ultra-short echo-time pulmonary MRI: Evaluation and reproducibility in COPD subjects with and without bronchiectasis. J Magn Reson Imaging 41:1465–1474
12. Dournes G, Grodzki D, Macey J et al (2015) Quiet submillimeter MR imaging of the lung is feasible with a PETRA sequence at 1.5 T. Radiology 276:258–265
13. Tiddens HAWM, Stick SM, Wild JM et al (2015) Respiratory tract exacerbations revisited: ventilation, inflammation, perfusion, and structure (VIPS) monitoring to redefine treatment. Pediatr Pulmonol 50:S57–S65
14. Bauman G, Puderbach M, Heimann T et al (2013) Validation of fourier decomposition MRI with dynamic contrast-enhanced MRI using visual and automated scoring of pulmonary perfusion in young cystic fibrosis patients. Eur J Radiol 82:2371–2377
15. van Beek EJR, Hill C, Woodhouse N et al (2007) Assessment of lung disease in children with cystic fibrosis using hyperpolarized 3-Helium MRI: comparison with shwachman score, chrispin-Norman score and spirometry. Eur Radiol 17:1018–1024
16. Stadler A, Stiebellehner L, Jakob PM et al (2007) Quantitative and o(2) enhanced MRI of the pathologic lung: findings in emphysema, fibrosis, and cystic fibrosis. Int J Biomed Imaging 2007:23624
17. Ciet P, Tiddens HAWM, Wielopolski PA et al (2015) Magnetic resonance imaging in children: common problems and possible solutions for lung and airways imaging. Pediatr Radiol. doi:10.1007/s00247-015-3420-y
18. Attariwala R, Picker W (2013) Whole body MRI: improved lesion detection and characterization with diffusion weighted techniques. J Magn Reson Imaging 38:253–268
19. Luna A, Sánchez-Gonzalez J, Caro P (2011) Diffusion-weighted imaging of the chest. Magn Reson Imaging Clin N Am 19:69–94
20. Gaviani P, Schwartz RB, Hedley-Whyte ET et al (2005) Diffusion-weighted imaging of fungal cerebral infection. Am J Neuroradiol 26:1115–1121
21. Moritani T, Kim J, Capizzano AA et al (2014) Pyogenic and non-pyogenic spinal infections: emphasis on diffusion-weighted imaging for the detection of abscesses and pus collections. Br J Radiol 87:20140011
22. Qi J, Olsen NJ, Price RR et al (2008) Diffusion-weighted imaging of inflammatory myopathies: polymyositis and dermatomyositis. J Magn Reson Imaging 27:212–217
23. Ream JM, Dillman JR, Adler J et al (2013) MRI diffusion-weighted imaging (DWI) in pediatric small bowel Crohn disease: correlation with MRI findings of active bowel wall inflammation. Pediatr Radiol 43:1077–1085
24. Miller MR, Hankinson J, Brusasco V et al (2005) Standardisation of spirometry. Eur Respir J 26:319–338

25. Tepper LA, Ciet P, Caudri D et al (2015) Validating chest MRI to detect and monitor cystic fibrosis lung disease in a pediatric cohort. Pediatr Pulmonol. doi:10.1002/ppul.23328
26. Tepper LA, Utens EMWJ, Caudri D et al (2013) Impact of bronchiectasis and trapped air on quality of life and exacerbations in cystic fibrosis. Eur Respir J 42:371–379
27. Liu H, Liu Y, Yu T, Ye N (2010) Usefulness of diffusion-weighted MR imaging in the evaluation of pulmonary lesions. Eur Radiol 20: 807–815
28. Tanaka R, Horikoshi H, Nakazato Y et al (2009) Magnetic resonance imaging in peripheral lung adenocarcinoma: correlation with histopathologic features. J Thorac Imaging 24:4–9
29. Uto T, Takehara Y, Nakamura Y et al (2009) Higher sensitivity and specificity for diffusion-weighted imaging of malignant lung lesions without apparent diffusion coefficient quantification. Radiology 252:247–254
30. Cohen J (1988) Statistical power analysis for the behavioral sciences, 2 edn. Routledge
31. Geert V, Molenberghs G (2000) Linear mixed models for longitudinal data, 1st edn. doi:10.1007/978-1-4419-0300
32. Burnham KP (2004) Multimodel Inference: understanding AIC and BIC in model selection. Sociol Methods Res 33:261–304
33. Deng Y, Li X, Lei Y, Liang C, Liu Z (2015) Use of diffusion-weighted magnetic resonance imaging to distinguish between lung cancer and focal inflammatory lesions: a comparison of intravoxel incoherent motion derived parameters and apparent diffusion coefficient. Acta Radiol 1–8. doi:10.1177/0284185115586091
34. Le Bihan D (2008) Intravoxel incoherent motion perfusion MR imaging: a wake-up call. Radiology 249:748–752
35. Chavhan GB, Alsabban Z, Babyn PS (2014) Diffusion-weighted imaging in pediatric body MR imaging: principles, technique, and emerging applications. Radiographics 34:E73–E88